Research Article

Peng Zhang, Hongsen Zhang, Guo Cui, Xiaodong Yue, Jinjun Guo*, and David Hui

Effect of steel fiber on impact resistance and durability of concrete containing nano-SiO_2

https://doi.org/10.1515/ntrev-2021-0040
received May 26, 2021; accepted June 8, 2021

Abstract: Impact drop weight tests, rapid chloride migration coefficient tests, single-sided freeze–thaw tests, and mechanical property tests were performed to investigate the effect of the steel fiber (SF) content on the impact resistance and durability of concrete containing nano-SiO_2 (NS). A fixed NS content of 3% and six SF contents in a range of 0–2.5% by volume were used. The impact resistance was measured based on the number of blows (N1, N2) and the impact energy. The durability of concrete includes its freeze–thaw resistance and chloride ion penetration resistance, which were appraised by the chloride ion diffusion coefficient (CDC) and relative dynamic elastic modulus (RDM), respectively. The ductility ratio was used to predict the impact resistance of concrete containing NS with different SF contents, and a linear relation between this ratio and the impact energy (R^2 = 0.853) was found. The experimental results indicated that SF could greatly improve the impact resistance of concrete. The addition of 2.0% SF increased N1 and N2 by 106 and 169%, respectively. In addition, an appropriate SF content significantly improved the durability of the concrete, including its frost resistance (especially in the middle and late freezing–thawing cycles) and chloride ion penetration resistance. An SF content of 1.5% was the optimum, decreasing the CDC of nano-concrete by 17.1% and minimizing the RDM loss. Moreover, the 1.5% SF content increased the compressive strength of concrete containing NS by 18.5%, whereas an SF content of 2.0% increased the splitting tensile strength and flexural strength by 77 and 20%, respectively. Furthermore, when the SF content exceeded a certain value, the improvement effect on these properties began to decrease and even became negative.

Keywords: concrete, impact resistance, durability, steel fiber, nano-SiO_2

1 Introduction

Concrete has been widely used in civil construction engineering because of its excellent mechanical properties, good workability, and plasticity [1]. In recent years, with the rapid expansion of China's infrastructure construction and the continuous progress of urbanization, the demand for concrete has continued to increase [2]. However, the limitations of cementitious materials make ordinary concrete brittle, with a low tensile strength, durability, crack resistance, toughness, and impact resistance [3]. The service performances of numerous concrete buildings rapidly deteriorate before the structures reach the end of their design service life [4]. An appreciable number of concrete structures must be demolished before they reach half of their design service life because of the poor durability properties of ordinary concrete [5]. At the same time, there has been a trend toward ultra-high strength, ultra-high rise, and long service life characteristics for modern civil structures [1]. It is accepted that traditional concrete has become increasingly difficult to adapt to the requirements of modern civil structures.

Over the past few years, nanomaterials have been widely used because of the great improvement that they provide in the mechanical properties and durability of cementitious composites. Nanomaterials are defined as particles between 1 and 100 nm in size with a large specific surface area [6]. It is generally believed that the enhancement of specific area will provide a superior surface for chemical reactions, thus accelerating the pozzolanic reaction within the material [7]. The production of pozzolanic reactions can densify the concrete microstructure by reducing the porosity and improving the interfacial transition zone performance, which can greatly improve the durability and mechanical properties of

* **Corresponding author: Jinjun Guo,** School of Water Conservancy Engineering, Zhengzhou University, Zhengzhou, 450001, China, e-mail: guojinjun@zzu.edu.cn
Peng Zhang, Hongsen Zhang: School of Water Conservancy Engineering, Zhengzhou University, Zhengzhou, 450001, China
Guo Cui, Xiaodong Yue: Beijing Municipal Road & Bridge Group Co., Ltd., Beijing, 100032, China
David Hui: Department of Mechanical Engineering, University of New Orleans, New Orleans, LA 70148, United States of America

concrete [8,9]. In addition, nanomaterials have become more affordable with the development of production technologies, the price of NS is about US$ 2300 per ton, nano-$CaCO_3$ is US$ 500 per ton, and nano-Al_2O_3 is US$ 2000 per ton in China. Previous studies have shown that the amount of nanomaterials incorporated is very small (about 4 kg in 1 m^3 concrete) [10,11]. The excellent performance and acceptable price of nanomaterials have attracted considerable attention. In recent years, researchers have investigated the effects of different nanomaterials on concrete, such as nano-metakaolin, nano-TiO_2, nano-Al_2O_3, nano-Fe_2O_3, nano-$CaCO_3$, phosphorous slag, and graphene. [12–18]. Among these nanomaterials, nano-SiO_2 (NS) is the most widely studied and used material. Because of their hot activity, NS particles can accelerate the formation of calcium silicate hydrate (C–S–H) gel and the dissolution of tricalcium silicate, providing a nucleating location for the C–S–H inclusion [19]. Zhang *et al.* performed experiments to study the effects of steel fiber (SF) and NS on the durability of concrete and showed that incorporating NS significantly enhanced the cracking resistance, permeability resistance, freezing–thawing resistance, and carbonation resistance of concrete when the NS content was limited to a certain range [20]. A group of researchers conducted a rapid chloride penetration test, which showed that mixing 3 or 6% NS significantly improved the chloride ion penetration resistance of concrete by refining the pore structure of the cementitious matrix [21]. Zhao *et al.* investigated the influence of different NS contents on the durability of concrete and found that adding NS could improve the freezing–thawing resistance of concrete by reducing the capillary pores in concrete specimens [22]. Zhang *et al.* summarized the effect of NS on high-performance concrete (HPC) and concluded that adding NS could significantly enhance the mechanical properties and durability of HPC, including its compressive strength, flexural behavior, crack resistance, abrasion resistance, water anti-permeability, chloride permeability, resistance to high temperatures, frost resistance, and water absorption capacity [1]. Ganesh *et al.* studied the influence of NS on the properties of geopolymer mortar and concluded that 2% NS significantly improved the compressive strength, splitting tensile strength, bending strength, and fracture performance of geopolymer mortar [23]. So far, numerous studies have been conducted on the effect of NS on cementitious composites, most of which focused on their durability and mechanical properties.

The biggest challenges for traditional concrete are its low ductility and high fracture risk, which can shorten the service life and make structural safety a serious concern. Besides, the variation of temperature and relative humidity in the mixing process could produce tensile stress in early-age concrete, which will cause cracks, especially for ultra-high strength concrete [24]. However, because of the properties of nanomaterials and their strengthening mechanism in concrete, simply adding nanomaterials cannot improve the defects of traditional concrete. Therefore, even though the durability and mechanical properties of concrete are greatly improved by the addition of NS particles, the toughness, ductility, and crack resistance of concrete still need to be enhanced [25]. Over the past few decades, numerous types of fibers have been widely used in traditional concrete. The fibers commonly used in concrete include different types of synthetic fibers [26–29], natural fibers [30], carbon fibers [15,31], and glass fibers [32]. Compared with other fibers, SFs have obvious effects of strengthening, toughening, and cracking resistance on concrete, and SFs have the advantages of simple manufacturing technology, convenient construction, and relatively low price, and hence SFs are the most researched and widely used concrete fiber materials. Zhang *et al.* investigated the fracture performance of SF-reinforced concrete containing NS and concluded that the addition of 2% SF produced the greatest improvement in the fracture properties of HPC containing NS and fly ash [25]. Li *et al.* found that adding SF to lightweight aggregate concrete significantly enhanced its post-cracking ductility [33]. Liu *et al.* experimentally investigated the influences of rubber and SF on the flexural properties of concrete, and the results indicated that the addition of SF led to significant improvements in the crack resistance, flexural strength, and toughness of rubberized concrete [34]. Niu *et al.* proved that SF improved the frost resistance of concrete by optimizing the pore structure, and a 1.5% SF content could significantly reduce the deterioration process of the concrete under frost damage [35]. There are different opinions among researchers regarding the chloride penetration resistance of SF-reinforced concrete. A group of researchers have studied the durability of concrete mixed with SF and revealed that SF could slow down the diffusion of chloride ions in concrete samples and had a positive effect on the chloride ion penetration resistance of ordinary concrete [36]. However, other researchers found that the SF could increase the porosity at the interface between the SF and the matrix and provided an open pore structure for aggressive ions from outside [37]. Many tests have been conducted to investigate the properties of SF-reinforced concrete, most of which focused on its toughness, ductility, and durability.

As one of the most widely used building materials, concrete is typically used under quasi-static loading conditions. However, many concrete structures are frequently

subjected to extreme impact forces. These impact forces come in various forms, including the impact of a vehicle on a concrete pier in a traffic accident; the impact of a falling object; the impact of water or ships on offshore structures, hydraulic structures, or bridge structures; and the impact of an explosion during a war or terrorist attack [38]. Because of the poor energy absorption capacity and brittleness of concrete, these various forms of impact can cause great harm to the safety and durability of a concrete structure [39]. To overcome the drawbacks of impact forces, researchers have proposed enhancing the impact resistance of traditional concrete by adding discontinuous short fibers. In recent years, SF [40], polypropylene fibers [41], polyvinyl alcohol fibers [42], carbon fibers [43], and other fibers have been widely studied as additives. The results have shown that adding various fibers can provide significant resistance to crack propagation in the cement matrix and enhance the impact resistance of concrete under static and impact loads. Compared with other fibers, SF has a more significant improvement effect on the mechanical properties and impact resistance of concrete because of its high strength and toughness; therefore, adding SF into the concrete matrix can provide higher ductility and deformability [44].

Recently, a growing number of studies have focused on the effects of NS particles on the mechanical properties and durability of concrete, and numerous studies have considered the effects of SF on the durability and cracking resistance of concrete. However, systematic investigations on the impact resistance and durability of concrete with the simultaneous additions of SF and NS are still lacking. This study utilized an NS content of 3%, along with six SF contents in the range of 0–2.5% by volume. Impact drop weight tests, rapid chloride migration coefficient tests, single-sided freeze–thaw tests, and mechanical property tests were carried out to study the effect of the SF content on the impact resistance and durability of concrete containing NS. A linear relationship between the ductility ratio and impact energy was established, which was perhaps the first time that the ductility ratio has been linked to the impact energy. This study had the goal of elucidating the SF-reinforcing mechanisms and providing design guidance for practical engineering applications of SF-reinforced concrete containing NS.

Table 1: Composition of cement (%)

SiO_2	Al_2O_3	Fe_2O_3	CaO	MgO	Na_2O	K_2O	SO_3
21.05	5.28	2.57	63.14	3.58	0.17	0.58	2.39

Table 2: Composition of fly ash (%)

SiO_2	Al_2O_3	Fe_2O_3	CaO	MgO	Na_2O	K_2O	SO_3
52.12	17.86	6.57	9.12	3.26	2.38	2.05	0.23

2 Experimental program

2.1 Raw materials

P·I 42.5 Portland cement, produced by Shandong Lucheng Cement Co., Ltd., and Class 1 fly ash, produced by Luoyang power plant, were used in this study. Their compositions and properties are listed in Tables 1 and 2, respectively. Broken stones (with grain diameters ranging from 4.75 to 26.5 mm) were used as coarse aggregate (CA), and natural river sand with a fineness of 2.7 was used as fine aggregate (FA). In addition, a liquid superplasticizer (SP) with a water reducing ratio of 30% was used to improve the flowability of the concrete. The NS used in this study was produced by Wan Jing New Material Co., Ltd., Hangzhou City, and its appearance and properties are shown in Figure 1 and Table 3, respectively. Milling SF was chosen as the additive for the concrete specimens because it can effectively improve the bond strength of the fiber matrix, along with the flexural strength and toughness [45]. The appearance and properties of the SF are shown in Figure 2 and Table 4, respectively.

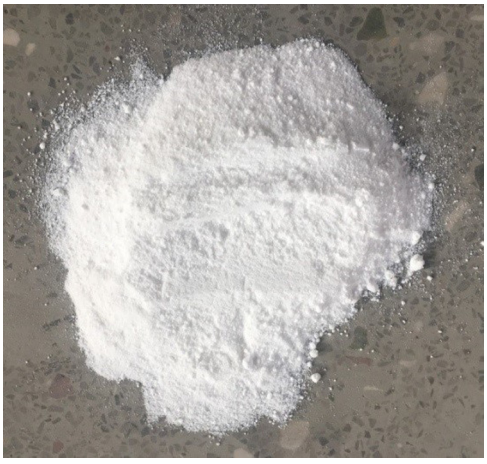

Figure 1: Image of NS.

Table 3: Properties of NS

Purity (%)	pH	Average particle size (nm)	Specific surface area (m^2/g)	Dry reduction (%)	Loss on ignition (%)	Stacking density (g/m^3)
99.6	6.2	30	200	1.0	1.0	0.054

Figure 2: Image of SFs.

2.2 Mix proportions and specimen preparation

Constant water-to-binder and sand ratios of 0.37 and 39% were used in this study, respectively. According to the related studies on fly ash, 15% of the weight of the cementitious material was replaced by fly ash to ensure the performance of the concrete [46,47]. A fixed NS content of 3% and six different SF volume fractions (0, 0.5, 1, 1.5, 2, and 2.5%) were used, as summarized in Table 5. Previous research indicated that adding nanomaterials to the water for mixing before it was added to the mixer could ensure that the nanomaterials were mixed uniformly [48]. Based on this, the NS particles and SP were added to the water for mixing, and this mixture was added to the mixer to obtain a better dispersion effect and reduce the adhesion of the nanomaterials to the mixer. The preparation process for the concrete specimens is given below.

First, SP and NS particles were added to the water for mixing. Then, the mixer was soaked with water. After the mixer was wetted, CA and FA were added and stirred for 60 s, followed by stirring with cement and fly ash for 60 s. Then, SF was added in the direction of the impeller of the mixer. After 30 s of stirring, the mixture of water, SP and NS were added to the mixer and mixed for 60 s, after which the remaining water was added and mixed for 60 s. Finally, the fresh mixture was poured into molds and compacted on a vibrating table. All the specimens were kept at ambient temperature for 24 h until demolding and then cured in a standard curing room for 28 days to reach the test age. The mixing process is shown in Figure 3.

2.3 Experimental methods

2.3.1 Mechanical property tests

Mechanical property tests were carried out according to the Chinese National Standard JT/G E30-2005. Three specimens were prepared for each mix ratio, and the mean value of the three results was obtained. Cube specimens (150 mm × 150 mm × 150 mm) were used for the compression tests, which were conducted in a hydraulic servo testing machine with a maximum bearing capability of 2000 kN. Beam specimens (100 mm × 100 mm × 400 mm) were used to evaluate the flexural behavior, which was tested using an antifracture testing machine. The splitting tensile strength was measured using a hydraulic servo testing machine with a maximum range of 1000 kN, and cube samples with a side length of 150 mm were used for this test.

2.3.2 Impact resistance test

The impact resistance test was carried out in accordance with the Chinese National Standard CECS 13-2009. An impact testing machine manufactured by Hualong Instrument Co., Ltd. was used. Five 150 mm × 150 mm × 150 mm cube specimens were prepared for each mix ratio. Figure 4 shows the

Table 4: Properties of SF

Length (mm)	Equivalent diameter (mm)	Length–diameter ratio	Tensile strength (MPa)
32.0	0.56	57.1	800.0

Table 5: Mix proportions of concrete specimens

Mixture no.	Water (kg/m^3)	Cement (kg/m^3)	Fly ash (kg/m^3)	FA (kg/m^3)	CA (kg/m^3)	NS (%)	SF (%)	SP (%)
Plain concrete (PC)	190	437	77	646	990	0	0	0
NS3-SF00	190	423.89	77	646	990	3	0	0.6
NS3-SF05	190	423.89	77	646	990	3	0.5	0.6
NS3-SF10	190	423.89	77	646	990	3	1.0	0.8
NS3-SF15	190	423.89	77	646	990	3	1.5	1.0
NS3-SF20	190	423.89	77	646	990	3	2.0	1.2
NS3-SF25	190	423.89	77	646	990	3	2.5	1.4

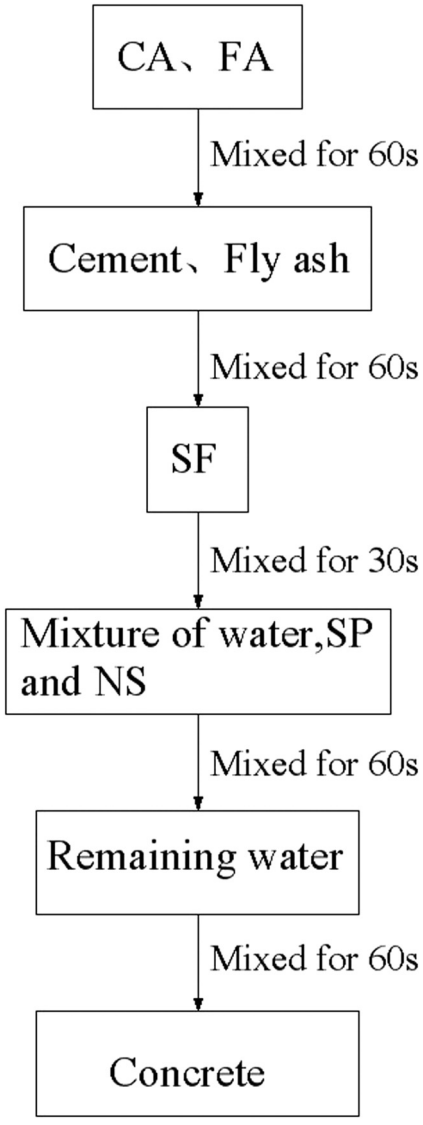

Figure 3: Mixing process of concrete.

apparatus used for the impact tests. Because of the large distribution of the impact resistance test data, the maximum and minimum values were removed, and the mean values of the remaining three test results were obtained. Before the test, the specimen was placed at the designated position on the bottom plate of the testing machine, and the testing machine was opened.

The test procedure was as follows. The drop weight was freely released from a certain height to impact the concrete specimen. The impact energy range of the free drop was 50–2000 J. To ensure the accuracy of the test results, the impact energy was set to 50 J. One impact process was defined as a cycle. After each cycle, the surfaces of the specimens were carefully observed. When the first visible crack appeared in the specimen, the number of blows was recorded as N1. The value of N2 was the number of blows required to reach the ultimate failure point when the crack width reached 1 mm.

2.3.3 Chloride ion penetration resistance test

To test the chloride ion penetration resistance of SF-reinforced concrete containing NS, the rapid chloride migration coefficient method (RCM) was adopted according to the Chinese National Standard JTG/T B07-01-2006. The testing instrument is shown in Figure 5. NaOH with a concentration of 0.3 mol/L was used as the anode solution, and 10% NaCl was used as the cathode solution. An external electric field was used to allow the chloride ions in the solution to migrate inside the specimen. At the end of the test, the final temperature and current of the anode solution were recorded. Finally, the specimen was split along the axis, and $AgNO_3$ solution was sprayed on the split section. $AgNO_3$ can react with chloride ions in the specimen to form AgCl, which can be precipitated out. Therefore, the permeation depth of the chloride ions could be determined based on the AgCl precipitation, and the diffusion coefficient of the chloride ions in the concrete was calculated. The chloride ion diffusion coefficient was calculated using Equation (1):

(a) (b)

Figure 4: Impact testing apparatus: (a) impact testing machine and (b) impact testing specimen.

$$D_{\mathrm{RCM}} = \frac{0.0239(273 + T)}{(U - 2)t}\left(X_{\mathrm{d}} - 0.0238\sqrt{\frac{(273 + T)LX_{\mathrm{d}}}{U - 2}}\right), \quad (1)$$

where D_{RCM} is the unsteady transfer coefficient of concrete, which is called the chloride diffusion coefficient; T is the average of the initial and final temperatures of the anode solution, °C; U is the test voltage, V; L is the thickness of the specimen, mm; X_{d} is the average chloride ion penetration depth, mm; and t is the test duration, h.

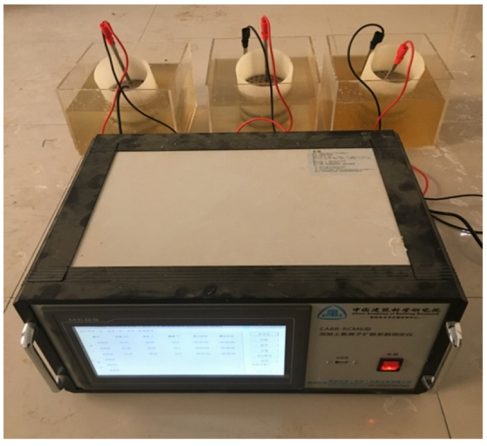

Figure 5: Instrument used for RCM test.

2.3.4 Frost resistance test

A single-sided freeze–thaw test, which could make the test environment closer to the actual freeze–thaw damage environment of a concrete structure, was adopted based on Chinese National Standard JGJ 55-2011, as shown in Figure 6. At the age of 28 days, cube specimens with a size of 150 mm × 110 mm × 70 mm were exposed to a 3.0% NaCl solution for freezing–thawing cycles. The frost resistance was measured based on the relative dynamic elastic modulus (RDM) after 4, 16, and 28 freezing–thawing cycles. Three concrete specimens were prepared for each mix ratio, and the mean value was used as the result. The RDM of the concrete specimens was calculated using the following equation (2):

Figure 6: Instrument used for frost resistance test.

$$\mathrm{RDM} = \frac{f_o^2}{f_n^2} \times 100\% \quad (2)$$

where f_o is the initial transverse fundamental frequency of the concrete specimen (Hz), and f_n is the transverse fundamental frequency of the concrete specimen after n freeze–thaw cycles (Hz).

3 Results and discussion

3.1 Mechanical properties

As demonstrated in Figure 7a, the compressive strength first increased and then decreased with increasing SF content, and 2.0% was considered to be the optimal SF content. The compressive strength of the concrete with the optimal SF content was 18.5% better than that without SF. This could be explained by the following two points: On one hand, the NS particles filled the micropores inside the concrete, increased the concrete density, and accelerated the formation of the C–S–H gel [49]; on the other hand, the incorporation of SF into the concrete further increased the density and stiffness, and restrained the propagation of microcracks before the concrete reached the ultimate strength [44]. However, increasing the SF content could not continuously enhance the compressive strength of concrete because excess SF caused mixing difficulty and fiber balling, which adversely affected the workability and uniformity [50].

With increasing SF content, the flexural and splitting tensile strengths first increased and then decreased, and the optimal SF content for both was 1.5%, as shown in Figure 7b and c. The flexural strength of the nano-concrete with the optimal SF content was 20.0% better than the concrete without SF, and the splitting tensile strength was 77.5% better. The improvement of fibers on splitting tensile strength was because the evenly distributed fibers could act as stitches between two cracked parts to transfer the stresses and improve the tensile capacity [51]. Because a previous study showed that increasing the fiber content could decrease the average distance between the fibers, and the increased fibers shared the load, thus reducing the average bonding stress between the fibers and the matrix [52]. This lower average bonding stress could effectively restrain the expansion of cracks, thus enhancing the splitting tensile strength and flexural strength.

Figure 8 presents the flexural failure patterns of concrete specimens with and without SF. As shown in

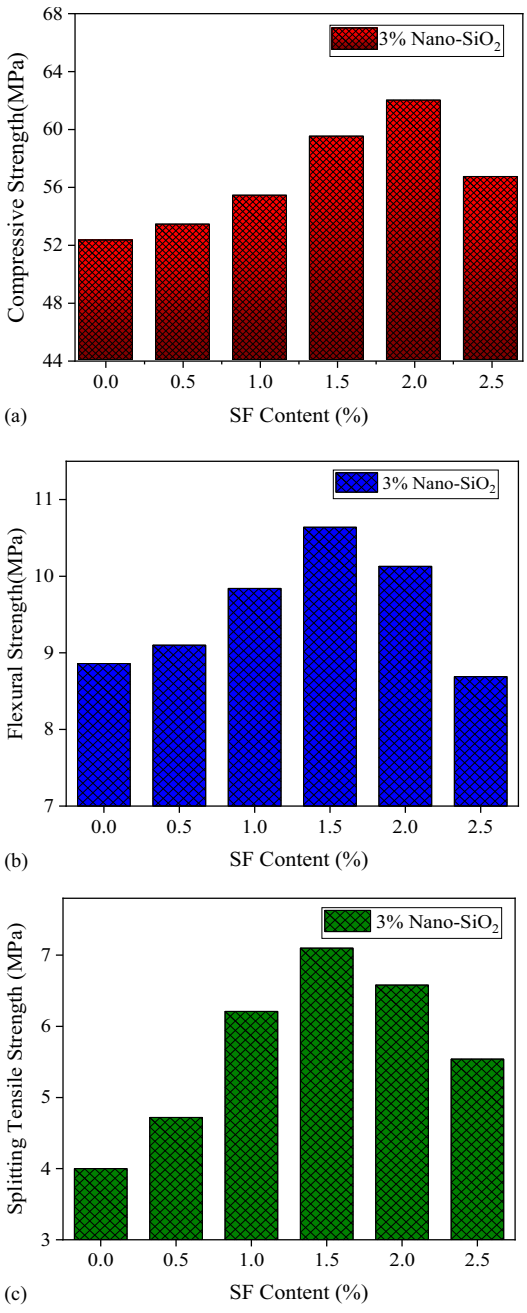

Figure 7: Effect of SF on mechanical strengths: (a) compressive strength, (b) flexural strength, and (c) splitting tensile strength.

Figure 8, with an increase in the SF content from 0 to 1.5%, the flexural failure pattern of the concrete specimen changed from brittle to ductile, and the damaged specimen was relatively complete, with only visible cracks appearing on the surface. However, a high fiber content does not always give concrete good ductility, but a threshold exists [53]. Excessive fiber leads to an increase in the internal pores in the matrix and a decrease in strength.

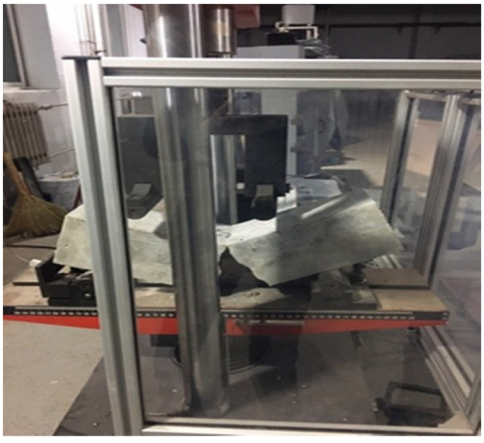

(a)

(b)

Figure 8: Flexural failure patterns of nano-concrete specimens: (a) specimen without SF and (b) specimen with 1.5% SF.

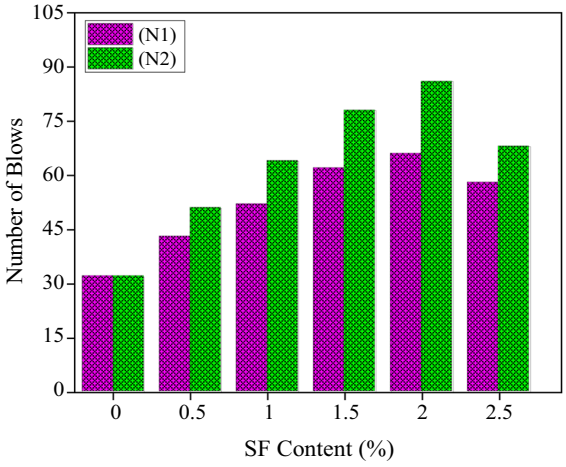

Figure 9: Influence of SF content on number of blows of concrete mixed with 3% NS.

3.2 Impact resistance

The numbers of blows required for the first visible crack to appear and for the ultimate failure were recorded as N1 and N2, respectively. The impact energy of each blow was constant at 50 J; thus, the impact energy was equal to 50 × N*i* (*i* = 1 or 2). Figures 9 and 10 show the variation in the blow numbers and impact energy of the nano-concrete at the first crack stage and failure stage with the change in the SF content, respectively. The SF significantly enhanced the impact resistance of the concrete in both the stages. The impact resistance of the specimens first increased and then decreased with the variation in the SF content from 0 to 2.5%, and 2.0% was the optimal SF content. The numbers of blows (or impact energy values) at the first crack and failure stages of the nano-concrete with the optimal SF content were improved by 106 and 169%, respectively, compared with nano-concrete without SF. This was because the incorporation of SF into nano-concrete can form a three-dimensional network structure, making nano-concrete more compact and effectively enhancing its anti-cracking ability under impact. When the specimen cracked under the impact of the drop hammer, the bridging action of the SF across the cracks inhibited or slowed down the expansion of the cracks and enhanced the toughness and impact resistance of the concrete [54]. As a result, a larger number of blows (or impact energy) was required to break the bond between the fibers and concrete matrix, which resulted in the pull-out of the SFs and ultimate failure of the specimens [55].

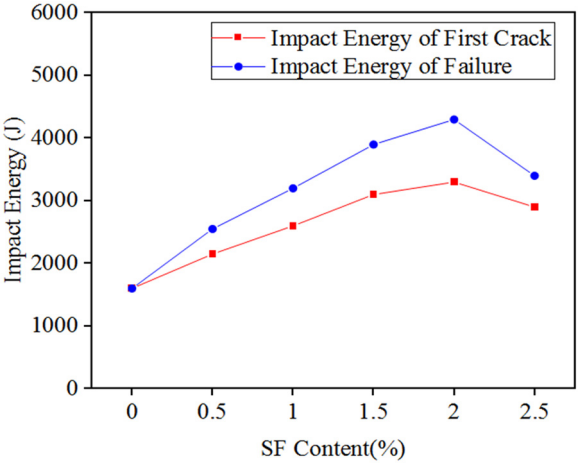

Figure 10: Effect of SF content on impact energy of concrete mixed with 3% NS.

Figure 11 shows the observed failure patterns of the concrete mixed with SF contents of 0 and 1.5%. As shown in Figure 11a, the failure of the specimen occurred suddenly after the formation of the first crack, and after another one or two blows, the cracks became wider and extended to the edge of the specimen, dividing the specimen into two parts, as described in previous studies [38,40,56]. This indicated that the addition of NS did not change the brittleness of the concrete. However, because of the bridging action of the SF, the failure pattern of the concrete mixed with 1.5% SF was relatively complete. The crack did not extend to the bottom of the specimen, and the overall internal structure was not destroyed, as shown in Figure 11b.

Ductility refers to the deformation capacity before failure under loads. It is typically used to measure the tensile and bending properties of cement-based cementitious materials. Extending this definition to the impact resistance, ductility ratio is defined as the ratio of the number of blows at the failure stage (N2) to the number of blows at the cracking stage (N1) [57]. Figure 12 shows the correlation between the impact energy and the ductility ratio. According to the empirical equations developed, the impact energy may be linearly correlated with the ductility ratio with a maximum coefficient of determination (R^2 = 0.853), which means that a higher ductility ratio corresponds to a greater impact resistance, whereas specimens with higher SF volume fractions do not always obtain higher ductility ratios, similar to the impact resistance. This is because the excessive SF is not evenly dispersed in the concrete, and the increase in specific surface area leads to a relative shortage of cementitious material, increasing the internal micro-cracks of the concrete, and thus reducing its impact resistance [58]. This model could be used to predict the impact resistance of concrete with different SF contents.

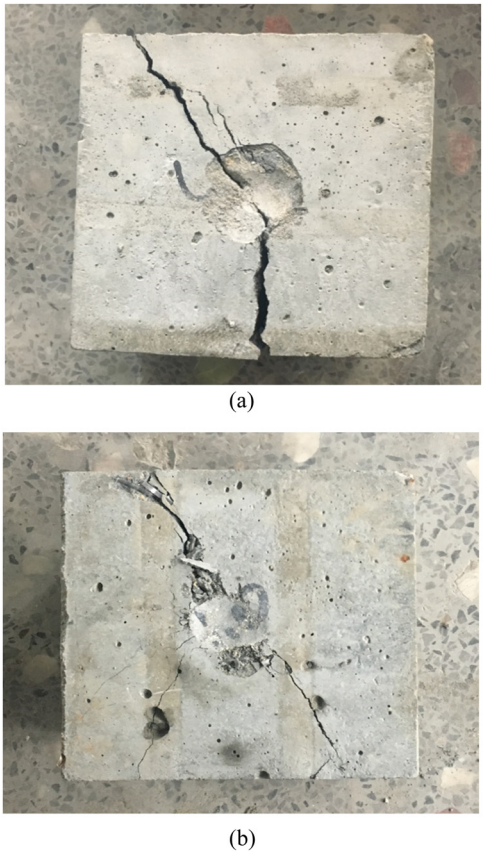

Figure 11: Impact failure patterns of nano-concrete specimens: (a) specimen without SF and (a) specimen with 1.5% SF.

3.3 Chloride ion penetration resistance

Cracking seriously affects the impermeability and resistance of concrete to the penetration of external harmful ions. The cracks in concrete will accelerate the transmission of corrosive media and the corrosion of steel bars, which will aggravate the degradation of concrete properties [59]. Porosity is another key factor affecting the chloride ion penetration resistance of concrete, and a denser cement paste and lower porosity result in better chloride ion penetration resistance. The pores in concrete can be classified into four types: harmless pores (aperture <20 nm), less harmful pores (20 nm ≤ aperture ≥ 50 nm), harmful pores (50 nm ≤ aperture ≥ 200 nm), and very harmful pores (aperture ≥ 200 nm) [60]. Zhao *et al.* experimentally studied the influencing factors of water transport and distribution in cement-based materials [61]. Zhang and Li studied the effect of distribution and interconnection of pores or cracks on the durability of

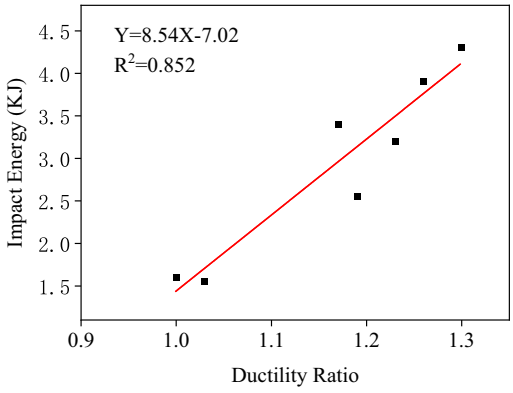

Figure 12: Correlation between impact energy and ductility ratio.

concrete [62]. From their research, it can be concluded that the distribution and interconnection of pores and cracks influence the water transport and distribution in cement-based materials, which seriously affect the permeability of cement-based cementitious materials. Previous studies have indicated that the filling effect and nucleation effect of NS could improve the compactness of concrete by promoting the hydration of cement [63]. In addition, the addition of nanomaterials can refine the pore structure, reduce the number of very harmful pores, and transform harmful pores into harmless pores in concrete [64,65]. These studies also indicated that the incorporation of NS could significantly decrease the chloride diffusion coefficient.

Figure 13 shows the effect of the SF content on the mean chloride ion diffusion coefficient (CDC) of concrete mixed with 3% NS. The mean CDC first decreased and then increased when the SF content varied from 0 to 2.5%, and the optimal content of SF was 1.5%. The mean CDC of nano-concrete with the optimal SF content was 17.1% lower than that of nano-concrete without SF. This was because the incorporation of SF into the concrete could inhibit the growth and propagation of cracks, thereby improving the structural durability [66]. In addition, the incorporation of SF enhanced the corrosion resistance of the concrete by reducing its porosity and breaking the permeation channel of chloride ions. However, this test was influenced by the current passing through the concrete surface. As a conductive element, SF significantly accelerated the chloride diffusion rate of the concrete. On the other hand, Frazão *et al.* found that the protective oxide film of SF was thinned by the accumulation of chloride ions at the fiber–matrix interface, thus weakening the corrosion resistance of the concrete [67]. This conclusion was also supported by Afroughsabet *et al.* [37]. Therefore, the influence of SF on the chloride ion penetration resistance of concrete was not prominent. Finally, as previously mentioned, the addition of excessive SF increased the number of cracks in the concrete, allowing aggressive chloride ions to penetrate the concrete through these cracks, which reduced the chloride ion penetration resistance of the concrete.

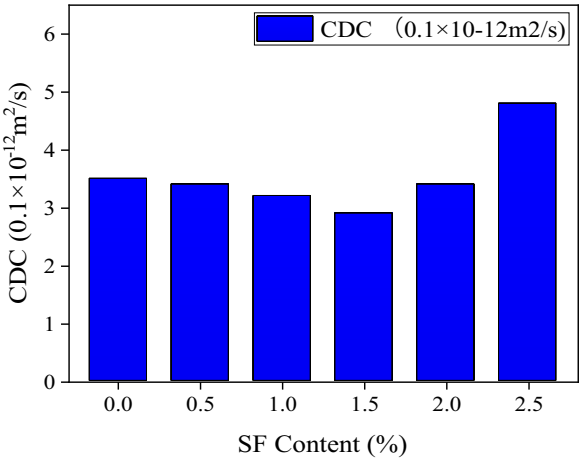

Figure 13: Effect of SF content on chloride diffusion coefficient of concrete mixed with 3% NS.

3.4 Frost resistance

Figure 14 illustrates the curve of mean RDM loss with the number of freezing–thawing cycles. With the SF content increase, the RDM loss first decreases and then increases, and the optimal content is 1.5%. As the number of freezing–thawing cycles increased, the RDM loss increased. After 4, 16, and 28 freezing–thawing cycles, the mean RDM loss of specimens with optimal SF content is 3.4, 8.7, and 11.8%, while the mean RDM loss of nano-concrete specimens without SF is 6, 15.9, and 27.2%, respectively. Moreover, with the increase of freezing–thawing cycles, the RDM loss rate of the specimens decreased significantly, which is shown in Figure 14 as the slope of the curve gradually decreased.

The pore structure parameters, including the porosity, average air void diameter, pore size distribution, air content, and spacing coefficient of air voids, are generally believed to be the main factors affecting the frost resistance of concrete [68]. The first few freezing–thawing cycles had little effect on the RDM loss because the internal damage to the specimen was relatively small at this time, and frozen water in the pores generated by the freezing–thawing cycles could compress the concrete and increase its density. With an increase in the number of freezing–thawing cycles, the freezing–thawing damage to the concrete was aggravated. Cracks developed rapidly, and the porosity was high. At this time, a large amount of frozen water in the pores compressed the concrete, accelerating the freeze–thaw damage. However, the result in Figure 14 shows that with the increase of freezing–thawing cycles, the RDM loss rate of the specimens decreased significantly, and the slope of the curve gradually decreased, which is the opposite of the theoretical pattern of destruction. This could be attributed to the following two reasons. First, the SF could not inhibit the generation of cracks in the early stage of the test but could suppress their propagation [69]. Second, in the middle and late periods of the freezing–thawing cycles, when the concrete was

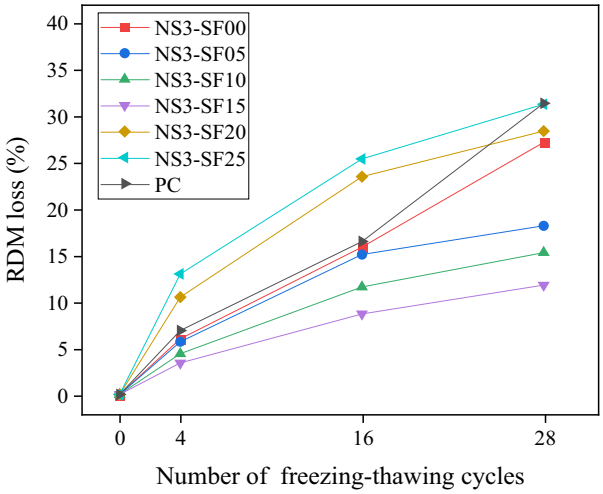

Figure 14: Effect of SF content on relative dynamic modulus after freeze–thaw cycles.

compressed by the frozen water in the pores, the SF could bear the frost resistance-induced tensile stress on the matrix, inhibit the further expansion of cracks, and limit the freezing–thawing damage to the matrix [70]. As previously mentioned, the SF could inhibit the growth and propagation of cracks and thus improve the structural durability [64]. It is easy to conclude that adding an appropriate amount of SF greatly improves the frost resistance of nano-concrete, especially in the middle and late periods of the freezing–thawing cycles. However, with a continuous increase in SF, the RCM loss increased sharply, and the frost resistance of the nano-concrete also showed a trend to sharply decline, even worse than that of PC.

Figure 15 shows the surface damage of nano-concrete mixed with 1.5% SF and 2.5% SF after 28 freezing–thawing cycles. Obviously, the nano-concrete with the 1.5% SF volume fraction has a relatively complete appearance with little surface peeling, while the surface of the specimen with the 2.5% SF content is uneven, with severe peeling, and exposed CA and fiber can even be seen. This may have been due to the excessive SF causing a relative shortage and the increase in porosity of cementing material, with the increased primary defects of the concrete allowing water to enter the matrix through these pores, accelerating the freeze–thaw damage to the concrete.

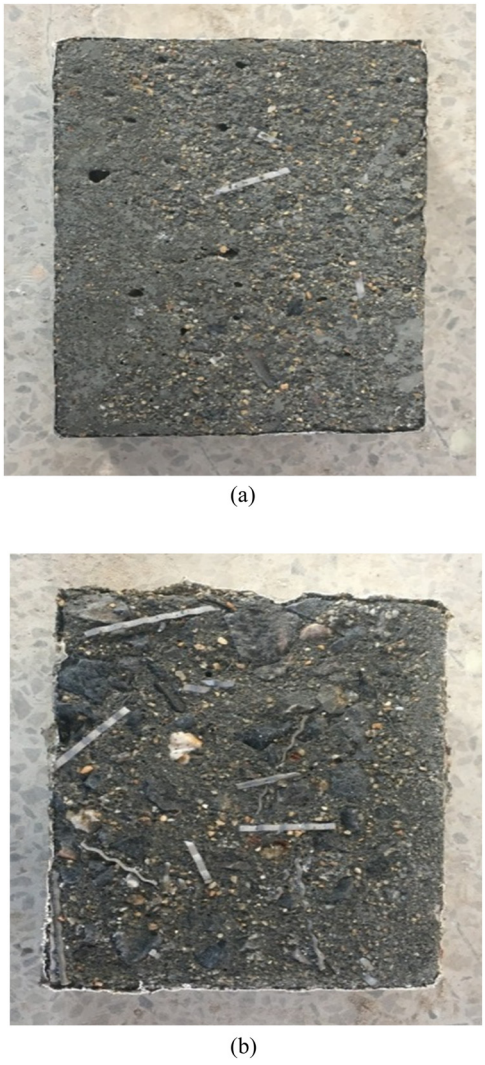

Figure 15: Surface damage of nano-concrete specimens: (a) specimen with 1.5% SF and (b) specimen with 2.5% SF.

4 Conclusion

The experimental results of tests to determine the impact resistance, chloride ion penetration resistance, frost resistance, and mechanical properties of SF-reinforced concrete containing NS were reported in this study. Based on the experimental results described herein and combined with the failure patterns of the specimens, the mechanism of the SF effect was analyzed, and the following conclusions were drawn.

(1) Incorporating SF could significantly improve the impact resistance of concrete containing NS. An SF content of 2.0% increased N1 and N2 by 106 and 169%, respectively. However, an excessive SF content had an adverse effect on the impact resistance of concrete containing NS. A linear relationship between the ductility ratio and impact energy was established, and the R^2 value was 0.853, which could be used to predict the impact resistance of concrete with different SF contents.

(2) The addition of an appropriate amount of SF had a positive effect on the durability of the concrete, including its chloride penetration resistance and freezing–thawing resistance (especially in the middle and late freezing–thawing cycles). An SF content of 1.5% was considered the optimum. On one hand, it could decrease the mean CDC of nano-concrete by 17.1%; on the other hand, 1.5% SF could minimize the mean RDM loss. The mean RDM losses were only 3.4, 8.7, and 11.8% after 4, 16, and 28 freeze–thaw cycles, respectively. However, when the SF content exceeded 1.5%, the durability of concrete containing NS showed an obvious declining trend.
(3) The mechanical properties of the nano-concrete were enhanced to different degrees by incorporating SF. The 1.5% SF content increased the compressive strength of concrete by 18.5%, whereas an SF content of 2.0% increased the splitting tensile strength and flexural strength by 77 and 20%, respectively. However, increasing the SF content could not continuously enhance the mechanical properties of concrete containing NS, and an excessive SF content negatively affected the impact resistance of concrete containing NS.

Funding information: The authors would like to acknowledge the financial support received from the National Natural Science Foundation of China (Grant No. 51979251, U2040224), the Natural Science Foundation of Henan (Grant No. 212300410018), and Program for Innovative Research Team (in Science and Technology) in University of Henan Province of China (Grant No. 20IRTSTHN009).

Author contributions: All authors have accepted responsibility for the entire content of this manuscript and approved its submission.

Conflict of interest: David Hui, who is the co-author of this article, is a current Editorial Board member of *Nanotechnology Reviews*. This fact did not affect the peer-review process. The authors declare no other conflict of interest.

References

[1] Zhang P, Wan JY, Wang KL, Li QF. Influence of nano-SiO_2 on properties of fresh and hardened high performance concrete: a state-of-the-art review. Constr Build Mater. 2017;148:648–58.
[2] Wang YG, Hughes P, Niu HC, Fan YH. A new method to improve the properties of recycled aggregate concrete: composite addition of basalt fiber and nano-silica. J Clean Prod. 2019; 236:117602.
[3] Zhang P, Li QF, Zhu HT, Zhang TH. Fracture toughness of nano-SiO_2 and steel fiber reinforced concrete. J Build Mater. 2017; 20:366–72. (in Chinese).
[4] Ahmed SFU, Mihashi H. A review on durability properties of strain hardening fibre reinforced cementitious composites (SHFRCC). Cem Concr Compos. 2007;29(5):365–76.
[5] Zhang P, Li QF, Wang J, Shi Y, Ling YF. Effect of PVA fiber on durability of cementitious composite containing nano-SiO_2. Nanotechnol Rev. 2019;8(1):16–127.
[6] Balapour M, Joshaghani A, Althoey F. Nano-SiO_2 contribution to mechanical, durability, fresh and 7 characteristics of concrete: a review. Constr Build Mater. 2018;181:27–41.
[7] Jagadesh P, Ramachandra Murthy A, Murugesan R. Effect of processed sugar cane bagasse ash on mechanical and fracture properties of blended mortar. Constr Build Mater. 2020; 262:120846.
[8] Ling Y, Zhang P, Wang J, Taylor P, Hu S. Effects of nanoparticles on engineering performance of cementitious composites reinforced with PVA fibers. Nanotechnol Rev. 2020;9(1):504–14.
[9] Balapour M, Ramezanianpour A, Hajibandeh E. An investigation on mechanical and durability properties of mortars containing nano and micro RHA. Constr Build Mater. 2017; 132:470–7.
[10] Zeng WL, Zhao YX, Zheng HB, Poon CS. Improvement in corrosion resistance of recycled aggregate concrete by nano silica suspension modification on recycled aggregates. Cem Concr Compos. 2020;106:103476.
[11] Li WG, Luo ZY, Long C, Wu CQ, Duan WH, Shah SP. Effects of nanoparticle on the dynamic behaviors of recycled aggregate concrete under impact loading. Mater Des. 2016;112:58–66.
[12] Muhd Norhasri MS, Hamidah MS, Mohd Fadzil A, Megawati O. Inclusion of nano metakaolin as additive in ultra high performance concrete (UHPC). Constr Build Mater. 2016;127:167–75.
[13] Joshaghani A, Balapour M, Mashhadian M, Ozbakkaloglu T. Effects of nano-TiO_2, nano-Al_2O_3, and nano-Fe_2O_3 on rheology, mechanical and durability properties of self-consolidating concrete (SCC): an experimental study. Constr Build Mater. 2020;245:118444.
[14] Liu CJ, He X, Deng XW, Wu YY, Zheng ZL, Liu J, et al. Application of nanomaterials in ultra-high-performance concrete: a review. Nanotechnol Rev. 2020;9(1):1427–44.
[15] Liu R, Xiao HG, Geng JS, Du JJ, Liu M. Effect of nano-$CaCO_3$ and nano-SiO_2 on improving the properties of carbon fibre-reinforced concrete and their pore-structure models. Constr Build Mater. 2020;244:118297.
[16] Wang L, Guo FX, Lin YQ, Yang HM, Tang SW. Comparison between the effects of phosphorous slag and fly ash on the C–S–H structure, long-term hydration heat and volume deformation of cement-based materials. Constr Build Mater. 2020;250: 118807.
[17] Wang J, Xu YQ, Wu XP, Zhang P, Hu SW. Advances of graphene- and graphene oxide-modified cementitious materials. Nanotechnol Rev. 2020;9(1):465–77.
[18] Ling YF, Zhang P, Wang J, Taylor P, Hu SW. Effects of nanoparticles on engineering performance of cementitious composites reinforced with PVA fibers. Nanotechnol Rev. 2020;9(1):504–14.

[19] Jo BW, Kim CH, Lim JH. Investigations on the development of powder concrete with nano-SiO_2 particles. KSCE J Civ Eng. 2007;11:37–42.
[20] Zhang P, Li QF, Chen YZ, Shi Y, Ling YF. Durability of steel fiber-reinforced concrete containing SiO_2 nano-particles. Materials. 2019;12(13):2184.
[21] Said AM, Zeidan MS, Bassuoni MT, Tian Y. Properties of concrete incorporating nano-silica. Constr Build Mater. 2012; 36:838–44.
[22] Zhao ZR, Kong J, Yang HX. Study on frost resistance of nano SiO_2 cement concrete. Appl Mech Mater. 2012;198–199:48–51.
[23] Ganesh P, Ramachandra Murthy A, Reheman MS. Mechanical, durability and fracture properties of nano modified FA-GGBS geopolymer mortar. Mag Concrete Res. 2020;72(4):207–16.
[24] Zhao HT, Jiang KD, Hong B, Yang R, Xu W, Tian Q, et al. Experimental and numerical analysis on coupled hygro-thermo-chemo-mechanical effect in early-age concrete. J Mater Civil Eng. 2021;33(5):04021064.
[25] Zhang P, Liu CH, Li QF, Zhang TH, Wang P. Fracture properties of steel fiber reinforced high performance concrete containing nano-SiO_2 and fly ash. Curr Sci India. 2014;106:980–7.
[26] Ling YF, Zhang P, Wang J, Chen YZ. Effect of PVA fiber on mechanical properties of cementitious composite with and without nano-SiO_2. Constr Build Mater. 2019;229:117068.
[27] Qin Y, Zhang XW, Chai JR. Damage performance and compressive behavior of early-age green concrete with recycled nylon fiber fabric under an axial load. Constr Build Mater. 2019;209:105–14.
[28] Du MR, Gao Y, Han GS, Li L, Jing HW. Stabilizing effect of methylcellulose on the dispersion of multi-walled carbon nanotubes in cementitious composites. Nanotechnol Rev. 2020;9(1):93–104.
[29] Qin Y, Zhang XW, Chai JR, Xu ZG, Li SY. Experimental study of compressive behavior of polypropylene-fiber-reinforced and polypropylene-fiber-fabric-reinforced concrete. Constr Build Mater. 2019;194:216–25.
[30] Naik D, Sharma A, Chada RR, Kiran R, Sirotiak T. Modified pullout test for indirect characterization of natural fiber and cementitious matrix interface properties. Constr Build Mater. 2019;208:381–93.
[31] Han JH, Wang DB, Zhang P. Effect of nano and micro conductive materials on conductive properties of carbon fiber reinforced concrete. Nanotechnol Rev. 2020;9(1):445–54.
[32] Ali B, Qureshi LA, Khan SU. Flexural behavior of glass fiber-reinforced recycled aggregate concrete and its impact on the cost and carbon footprint of concrete pavement. Constr Build Mater. 2020;262:120820.
[33] Li JJ, Wan CJ, Niu JG, Wu LF, Wu YC. Investigation on flexural toughness evaluation method of steel fiber reinforced lightweight aggregate concrete. Constr Build Mater. 2017;131: 449–58.
[34] Liu RY, Li H, Jiang QH, Meng XY. Experimental investigation on flexural properties of directional steel fiber reinforced rubberized concrete. Structures. 2020;27:1660–9.
[35] Niu DT, Jiang L, Bai M, Miao YY. Study of the performance of steel fiber reinforced concrete to water and salt freezing condition. Mater Des. 2013;44:267–73.
[36] Vincler JP, Sanchez T, Turgeon V, Conciatori D, Sorelli L. A modified accelerated chloride migration tests for UHPC and UHPFRC with PVA and steel fibers. Cem Concr Res. 2019; 117:38–44.
[37] Afroughsabet V, Biolzi L, Monteiro PJM. The effect of steel and polypropylene fibers on the chloride diffusivity and drying shrinkage of high-strength concrete. Compos Part B Eng. 2018;139:84–96.
[38] Abid SR, Abdul-Hussein ML, Ayoob NS, Ali SH, Kadhum AL. Repeated drop-weight impact tests on self-compacting concrete reinforced with micro-steel fiber. Heliyon. 2020; 6:e03198.
[39] Yoo DY, Banthia N. Impact resistance of fiber-reinforced concrete – a review. Cem Concr Compos. 2019;104:103389.
[40] Alavi Nia A, Hedayatian M, Nili M, Afrough Sabet V. An experimental and numerical study on how steel and polypropylene fibers affect the impact resistance in fiber-reinforced concrete. Int J Impact Eng. 2012;46:62–73.
[41] Banthia N, Gupta P, Yan C. Impact resistance of fiber reinforced wet-mix shotcrete – part 1: beam tests. Mater Struct. 1999;32(8):563–70.
[42] Xu B, Toutanji HA, Gilbert J. Impact resistance of poly(vinyl alcohol) fiber reinforced high-performance organic aggregate cementitious material. Cem Concr Res. 2010;40(2):347–51.
[43] Tabatabaei ZS, Volz JS, Baird J, Gliha BP, Keener DI. Experimental and numerical analyses of long carbon fiber reinforced concrete panels exposed to blast loading. Int J Impact Eng. 2013;57:70–80.
[44] Su CD, Lin HX. Mechanical performances of steel fiber reinforced high strength concrete disc under cyclic loading. Constr Build Mater. 2017;146:267–82.
[45] Wu ZM, Shi CJ, Khayat KH. Investigation of mechanical properties and shrinkage of ultra-high performance concrete: Influence of steel fiber content and shape. Compos Part B Eng. 2019;174:107021.
[46] Zhang P, Li QF. Effect of polypropylene fiber on durability of concrete composite containing fly ash and silica fume. Compos Part B Eng. 2013;45:1587–94.
[47] Golewski GL. The beneficial effect of the addition of fly ash on reduction of the size of microcracks in the ITZ of concrete composites under dynamic loading. Energies. 2021;14(3):668.
[48] Dong JM, Ma MB. Effect of dispersion method on the properties of nano-SiO_2 reinforced cement-based materials. Concrete. 2011;4:95–6. (in Chinese).
[49] Nazerigivi A, Najigivi A. Study on mechanical properties of ternary blended concrete containing two different sizes of nano-SiO_2. Compos Part B Eng. 2019;167:20–4.
[50] Ding Y, Bai YL. Fracture properties and softening curves of steel fiber-reinforced slag-based geopolymer mortar and concrete. Materials. 2018;11:1445.
[51] Wang L, He TS, Zhou YX, Tang SW, Tan JJ, Liu ZT, et al. The influence of fiber type and length on the cracking resistance, durability and pore structure of face slab concrete. Constr Build Mater. 2021;282:122706.
[52] Xu LH, Wu FH, Chi Y, Cheng P, Zeng YQ, Chen Q. Effects of coarse aggregate and steel fibre contents on mechanical properties of high performance concrete. Constr Build Mater. 2019;206:97–110.
[53] Kang ST, Lee Y, Park YD, Kim JK. Tensile fracture properties of an Ultra High Performance Fiber Reinforced Concrete (UHPFRC) with steel fiber. Compos Struct. 2010;92:61–71.

[54] Badr A, Ashour AF, Platten AK. Statistical variations in impact resistance of polypropylene fibre-reinforced concrete. Int J Impact Eng. 2006;32:1907–20.
[55] Abirami T, Loganaganandan M, Murali G, Fediuk R, Sreekrishna RV, Vignesh T, et al. Experimental research on impact response of novel steel fibrous concretes under falling mass impact. Constr Build Mater. 2019;222:447–57.
[56] Chen XY, Ding YN, Azevedo C. Combined effect of steel fibres and steel rebars on impact resistance of high performance concrete. J Cent South Univ Technol. 2011;18:1677–84.
[57] Mahakavi P, Chithra R. Impact resistance, microstructures and digital image processing on self-compacting concrete with hooked end and crimped steel fiber. Constr Build Mater. 2019;220:651–66.
[58] Pan HM, Ma YZ. Impact resistance steel fiber reinforced concrete and its mechanism of crack resistance and toughening. J Build Mater. 2017;20:956–61.
[59] Liu JP, Tian Q, Wang YJ, Li H, Xu W. Evaluation method and mitigation strategies for shrinkage cracking of modern concrete. Engineering. 2021;7(3):348–57.
[60] Zhang BL, Tan HB, Ma BG, Chen FJ, Lv ZH, Li X. Preparation and application of fine-grinded cement in cement-based material. Constr Build Mater. 2017;157:34–41.
[61] Zhao HT, Wu X, Huang YY, Zhang P, Tian Q, Liu JP. Investigation of moisture transport in cement-based materials using low-field nuclear magnetic resonance imaging. Mag Concrete Res. 2021;73(5):252–70.
[62] Zhang MH, Li H. Pore structure and chloride permeability of concrete containing nano-particles for pavement. Constr Build Mater. 2011;25:608–16.
[63] Li G, Zhou JC, Yue J, Gao X, Wang KJ. Effects of nano-SiO_2 and secondary water curing on the carbonation and chloride resistance of autoclaved concrete. Constr Build Mater. 2020; 235:117465.
[64] Zhang BL, Tan HB, Shen WG, Xu GL, Ma BG, Ji XL. Nano-silica and silica fume modified cement mortar used as surface protection material to enhance the impermeability. Cem Concr Compos. 2018;92:7–17.
[65] Wang L, Jin MM, Wu YH, Zhou YX, Tang SW. Hydration, shrinkage, pore structure and fractal dimension of silica fume modified low heat Portland cement-based materials. Constr Build Mater. 2021;272:121952.
[66] Pawad PY, Pand AM, Nagarnaik PB. Effect of steel fibers on modulus of elasticity of concrete. Int J Adv Eng Sci Technol. 2011;7:169–77.
[67] Frazão C, Camões A, Barros J, Gonçalves D. Durability of steel fiber reinforced self-compacting concrete. Constr Build Mater. 2015;80:155–66.
[68] Wang L, Guo FX, Yang HM, Wang Y, Tang SW. Comparison of fly ash, PVA fiber, Mgo and shrinkage-reducing admixture on the frost resistance of face slab concrete via pore structural and fractal analysis. Fractals. 2020;29:2140002–330.
[69] Yuan Y, Zhao RD, Li R, Wang YB, Cheng ZQ, Li FH, et al. Frost resistance of fiber-reinforced blended slag and Class F fly ash-based geopolymer concrete under the coupling effect of freeze-thaw cycling and axial compressive loading. Constr Build Mater. 2020;250:118831.
[70] Wang JB, Niu DT. Influence of freeze–thaw cycles and sulfate corrosion resistance on shotcrete with and without steel fiber. Constr Build Mater. 2016;122:628–36.